IEEE Access
Multidisciplinary : Rapid Review : Open Access Journal

Received January 29, 2021, accepted February 3, 2021, date of publication February 8, 2021, date of current version February 17, 2021.

Digital Object Identifier 10.1109/ACCESS.2021.3057998

Multiobjective Optimization Configuration of a Prosumer's Energy Storage System Based on an Improved Fast Nondominated Sorting Genetic Algorithm

FEI LI, XIANSHAN LI, BINQIAO ZHANG, ZHENXING LI, AND MINGFANG LU
College of Electrical Engineering and New Energy, China Three Gorges University, Yichang 443002, China

Corresponding author: Fei Li (97001455@qq.com)

This work was supported in part by the National Natural Science Foundation of China under Grant 52077120, in part by the Hubei Provincial Natural Science Foundation of China under Grant 2016CFA097, and in part by the Research Fund for Excellent Dissertation of China Three Gorges University under Grant 2021BSPY008.

ABSTRACT With the deepening of the ''source-load-storage'' interaction and the development of demand response technology, the emergence of prosumers has led to new vitality and potential for the optimal operation of microgrids. By implementing a demand response mechanism for prosumers, peak shaving and valley filling are realized, and load fluctuations are balanced. However, the high costs of investing and operating energy storage system (ESS) restrict their ability to participate in the scheduling of microgrids. In this paper, for the objectives of obtaining the lowest comprehensive costs and the smallest load fluctuations, an INSGA-II (Improved Fast Nondominated Sorting Genetic Algorithm) algorithm is proposed for the multiobjective configuration optimization model of a prosumer's ESS. To ensure the diversity of the population and improve the search ability of the algorithm in space, based on the original NSGA-II algorithm, the proportion factor set in the selection strategy is improved. The normal distribution crossover operator is introduced in the crossover process, and the local chaotic search strategy is added after the formation of the next generation of the population. An example of a science and technology park with five users is simulated and analyzed. Upon comparison with various typical intelligent algorithms, the results show that the performance of the improved NSGA-II algorithm is the best. At the same time, multiple calculation results show that the improved NSGA-II algorithm has strong algorithmic stability.

INDEX TERMS Prosumer, multiobjective optimization, INSGA-II, energy storage system configuration, comprehensive cost.

I. INTRODUCTION

At present, with the diversification of energy usage patterns and the pursuit of users' electricity experiences, prosumers with bidirectional power regulation characteristics are constantly emerging [1], and these has brought new vitality to modern microgrid optimization scheduling [2], [3]. Demand response technology is a powerful tool for the optimal dispatching of microgrids [4]–[7]. Ref. [4] presented a novel control algorithm for joint demand response management in microgrids to integrate renewable sources and reduce energy costs. Ref. [5] achieved a balance of energy deficiencies through a multi-microgrid alliance. Ref. [6] used game theory to study the interaction between an active distribution network and a microgrid containing prosumers. Ref. [7] realized the demand management of grid-connected microgrids through distributed control and human-in-the-loop optimization.

As prosumers have rich scheduling resources, such as photovoltaic storage, electric vehicles, and other forms of distributed energy storage devices, through the coordination of scheduling resources via demand response, the operational efficiency of prosumers can be greatly improved when participating in microgrid scheduling [8]. However, due to the high investment and operational costs of energy storage equipment in prosumers, the activities of prosumers participating

The associate editor coordinating the review of this manuscript and approving it for publication was Sonia F. Pinto.

in demand response are restricted, so these problems, such as the reasonable configuration of ESS and the orderly charging-discharging scheduling of prosumers, are gradually highlighted [9].

The ESS configuration for a prosumer in a microgrid is a mixed nonlinear programming and multiobjective optimization problem. At present, the common algorithms for multiobjective optimization are the strength Pareto evolutionary algorithm [10]–[12], multiobjective differential evolution algorithm [13], [14], and multiobjective particle swarm optimization algorithm [15], [16]. Among them, the principle of particle swarm optimization is simple and easy to implement. Ref. [17] used the particle swarm optimization algorithm to solve the problem of configuring the energy storage capacity in a microgrid. However, the particle swarm optimization algorithm has the problems of low search accuracy and easily falling into local optima. Ref. [18] used the enhanced Pareto evolutionary algorithm to solve the energy distribution problem of a microgrid, but the local search ability of the algorithm is poor. Ref. [19] improved the mutation strategy in the multiobjective differential evolution algorithm, which was used to solve the power generation capacity configuration problem of a wind-solar hybrid system. The optimization speed of the algorithm was improved. In short, the above algorithms generally have the problems of low search accuracy and slow convergence speed.

The NSGA-II algorithm was proposed by K. Deb *et al.* in 2002 based on the elite strategy of the fast nondominated sorting genetic algorithm [20]. By introducing the crowding distance method and elite strategy, NSGA-II can effectively ensure population diversity and improved global optimization ability. Compared with the ordinary genetic algorithm [21], its computational complexity is greatly reduced, thereby accelerating the Pareto front convergence process. At the same time, the independence of each optimization objective is maintained to the greatest extent possible. In view of the above advantages, the NSGA-II algorithm is very suitable for solving the mixed nonlinear multiobjective optimization problem in this paper. NSGA-II has been successfully applied to many power optimization problems, such as multiobjective reactive power optimization in power systems [22], the multiobjective optimization of integrated energy systems [23], and the multiobjective optimization of microgrids [24]–[26], and it has achieved good results.

Although the NSGA-II algorithm, as a classic multiobjective genetic algorithm, has been widely used, it still has room for improvement. For example, in the early stages of evolution, the dominant individual of the external elite population lacks elites, and the local search ability is weak. In this paper, a multiobjective optimization configuration model for a prosumer's ESS is established. Then, the original NSGA-II algorithm is improved from three aspects with regard to solving the model: the proportion factor in the selection strategy, the crossover operator and the local chaotic search strategy. Finally, we take a science and technology park with three typical users as a simulation example. According to the rigid load level and PV output in the park, the improved NSGA-II algorithm is used to complete the ESS configuration for the prosumer. Simulation results show that the improved NSGA-II algorithm can obtain a better Pareto solution set and better algorithmic stability than other algorithms (SPEA2, NSGA-II, NSGA-III).

II. THE PROSUMER ARCHITECTURE AND ITS SCHEDULING MECHANISM

A. TYPICAL STRUCTURE OF A PROSUMER

The typical structure of a prosumer is shown in Figure 1, including a load, a photovoltaic cell array, a photovoltaic DC/AC inverter, an ESS, and its bidirectional AC/DC converter. The demand response resources in microgrids with prosumers are mainly divided into four categories: photovoltaic, energy storage, load, and electricity price resources. During the operation of a microgrid, the four types of resources are closely combined. Thus, for prosumers, the capacity configuration of an ESS is not only influenced by the scheduling strategies of the microgrid but also related to the prosumer's demand response and price resources. The ESS of a prosumer can be used as a source or load for bidirectional energy exchange with the microgrid.

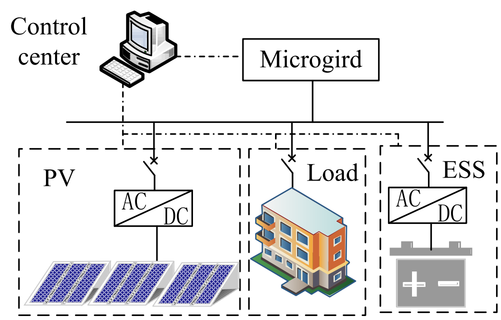

FIGURE 1. A microgrid system with a prosumer.

B. SCHEDULING MECHANISM OF A PROSUMER'S ESS

The configuration strategy for an ESS is shown in Figure 2.

According to the load level and the electricity price issued by the microgrid, by comprehensively considering the investment cost and operational cost of energy storage in the prosumer, the objective function of these costs and the load fluctuation is established to optimize power capacity and energy capacity and obtain the charging-discharging strategy for energy storage. It should be noted that, compared with a rigid load, a flexible load has a strong demand response ability, so it can respond to changes in the electricity price by adjusting its own load. Therefore, the configuration of ESS proposed in this paper mainly aims at the rigid loads of prosumers.

By comprehensively analyzing the photovoltaic output characteristics, load characteristics, ESS characteristics and time-of-use electricity prices of the system, the typical charging and discharging strategies for ESS of prosumers can be summarized as follows:

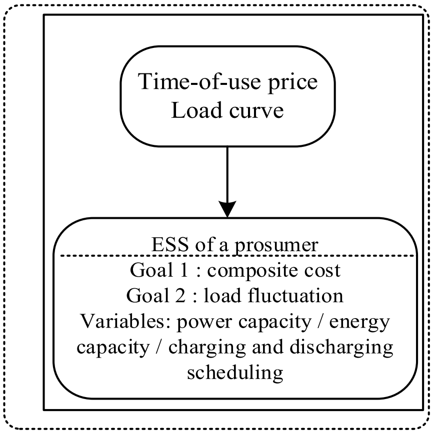

FIGURE 2. Multiobjective optimization model of energy storage for prosumers.

(1) During the mid-level electricity price periods in the early hours of the morning, the ESS battery discharges for the load, and the remaining load shortage is compensated by purchasing electricity from the microgrid.

(2) In the morning, if the PV output is more than the load, after meeting the load demand, the residual PV output is used to charge the ESS batteries; otherwise, after consuming all PV energies, the remaining load shortage is met by the microgrid. In this period, the ESS remains in the charging state until full.

(3) During the mid-level price periods in the afternoon, without any charging or discharging by the ESS, the load demand is supplied by the PV output, and the remaining load shortage is balanced by purchasing electricity from the microgrid.

(4) During the peak price periods at other times, as the PV output decreases to zero, the ESS batteries discharge power for the load until the SOC value drops to the minimum, and then the remaining load shortage is compensated by purchasing power from the microgrid.

III. ESS CONFIGURATION MODEL FOR A PROSUMER

Energy storage is a powerful tool to assist with the demand response of a prosumer, as it can enhance the active interaction between the prosumer and microgrid by optimizing their own electricity consumption behaviors and reduce electricity costs. In the current market, ESS are mainly made of lithium batteries. Due to the high prices of materials and complex manufacturing technology, it is difficult for a single user to bear the installation cost of a large-capacity ESS. Thus, when preparing to configure ESS for prosumers, it is necessary to design an effective capacity configuration model that considers the electricity price, investment cost and influence of load forecasting according to different application scenarios and prosumer demands.

As it is affected by many factors, the configuration of an ESS for a prosumer is a multiobjective optimization problem. The time sequence of the renewable energy generation and load adjustment in the microgrid lead to an increase of load fluctuation, which can be eliminated by the ESS to some extent. At the same time, the relatively high costs of installation and operation must be considered when optimizing the configuration of an ESS. In summary, this paper selects the comprehensive cost and the load fluctuation as the optimization objectives of the ESS configuration process for prosumers.

A. OBJECTIVE FUNCTION 1

The economic goal of the model considers the installation cost and operational cost of energy storage [27]. Therefore, the composite cost of energy storage system in a prosumer is defined as:

$$\begin{aligned}\min f1 &= I_{\text{inv}}^{DES} + O_{\text{Operator}}^{\text{DES}} \\ &= \frac{r}{1-(1+r)^{-Y}}\left(c_E^{\text{DES}} P_{\text{Cap}}^{DES} + c_E^{\text{DES}} E_{\text{Cap}}^{DES}\right) \\ &\quad + \sum_{t\in T}\left[\lambda_t\left(P_t^{\text{C}} - P_t^{\text{D}} + d_t - P_{v,t}\right)^{+}\right. \\ &\quad \left. + \theta_t\left(P_t^{\text{C}} - P_t^{\text{D}} + d_t - P_{v,t}\right)^{-}\right]\Delta t \end{aligned} \tag{1}$$

In Equation (1), λ_t represents the purchase price at time t, θ_t represents the repurchase price at time t, d_t represents the rigid load demand of the prosumer at time t, $P_{v,t}$ represents the photovoltaic output at time t, P_t^{C} represents the charging power of the prosumer at time t, P_t^{D} represents the discharging power of the prosumer at time t, P^{Cap} represents the maximum power capacity, E^{Cap} represents the maximum energy capacity, I_{inv}^{CES} represents the energy storage investment cost, $O_{\text{Operator}}^{\text{DES}}$ represents the energy storage operational cost, Y represents the service life of the ESS, γ represents the discount rate, $c_{\text{P}}^{\text{DES}}$ represents the investment cost per unit of power capacity, and $c_{\text{E}}^{\text{DES}}$ represents the investment cost per unit of energy capacity.

B. OBJECTIVE FUNCTION 2

Due to the large-scale integration of wind power, photovoltaics and other renewable energy sources, the intermittence of their outputs exacerbates load fluctuations, that may impact the stability of microgrid operation. Since the ESS has the ability of damping load fluctuations, which are used as the second optimization objective for the model, the corresponding function is expressed as follows:

$$f_2 = \sum_{t=1}^{24}(P_t^{\text{C}} - P_t^{\text{D}} + d_t - P_v - Pavg)^2 \tag{2}$$

$$P_{avg} = \frac{\sum_{t=1}^{24}(P_t^{\text{C}} - P_t^{\text{D}} + d_t - P_v)}{24} \tag{3}$$

In the formula, P_{avg} is the average equivalent load power.

C. CONSTRAINT CONDITIONS

The configuration of the ESS for prosumers needs to meet the SOC capacity constraints, the upper and lower limits of the capacity constraints and other conditions [27], which are as follows:

$$P_{\min}^{\mathrm{Cap}} \leq P^{\mathrm{Cap}} \leq P_{\max}^{\mathrm{Cap}} \tag{4}$$

$$E_{\min}^{\mathrm{Cap}} \leq E^{\mathrm{Cap}} \leq E_{\max}^{\mathrm{Cap}} \tag{5}$$

$$0 \leq P_t^{\mathrm{C}} \leq P^{\mathrm{Cap}} \tag{6}$$

$$0 \leq P_t^{D} \leq P^{\mathrm{Cap}} \tag{7}$$

$$E_0 = \mathrm{SOC}_0 \cdot E^{\mathrm{Cap}} \tag{8}$$

$$\mathrm{SOC}^{\min} \cdot E^{\mathrm{Cap}} \leq E_t \leq E^{\mathrm{Cap}} \tag{9}$$

$$E_t = E_{t-1} + \Delta t \left(\eta^c P_t^{\mathrm{C}} - \frac{P_t^{\mathrm{D}}}{\eta^d} \right) \tag{10}$$

In these equations, E_t represents the remaining energy capacity at time t, $\mathrm{SOC}^{\min}$ represents the lowest value of state-of-charge, η^c and η^d represent charging and discharging efficiency of all batteries, respectively.

The optimal power capacity and energy capacity of the ESS for prosumers are optimized based on the load of prosumer and the electricity prices. The optimal capacity model also optimizes the charging-discharging scheduling at each time interval:

$$[P^{\mathrm{Cap}}, E^{\mathrm{Cap}}, P_t^{\mathrm{C}}, P_t^{D}] = \min(f_1, f_2) \quad \text{s.t. Eq.(4)} \sim \text{Eq.(10)} \tag{11}$$

IV. THE NSGA-II ALGORITHM AND ITS IMPROVEMENT STRATEGY

A. PARETO OPTIMAL SET

There are great differences between multiobjective optimization and single-objective optimization. For the former, it is difficult to find a solution to optimize all the objective functions at the same time due to the conflicts between objectives. Therefore, there is usually a solution set, and its solutions cannot be compared with each other for all objective functions; these are called nondominated solutions or Pareto optimal solutions. In power systems, due to their complex operating environments, complex objective functions usually must be addressed. Because of the special mathematical form of the above model, it is difficult to obtain the analytical solution by using a numerical method, so an intelligent algorithm is introduced for complex models.

B. BASIC IDEAS OF THE NSGA-II ALGORITHM

The general process of the NSGA-II algorithm is as follows [20]: first, a population with N individuals, called the parent population, is randomly generated; then, nondominated sorting is used for the individuals in the population. Second, the crowding degree of the individuals is calculated, and this is used to classify their ranks. The appropriate individuals are selected by the selection operator and put into the mating pool, and the crossover and mutation operations are used to generate the new next-generation population. Finally, the superior individuals, as a new parent population, are obtained by the elite strategy operation; the above process is repeated until the termination condition is reached. The basic idea is as follows:

(1) Initialize a number of individuals, calculate the objective fitness of each initial individual according to the objective function under the condition of satisfying the constraints, and then perform nondominated sorting.

(2) Perform the process of the fast nondominated sorting algorithm. It needs to set two parameters when sorting. n_i represents the number of dominant individuals i among all individuals, and S_i represents the set of individuals dominated by individual i in the population. The steps of nondominated sorting are as follows:

Step 1: sort the nondominated individuals in the population according to the condition ($n_i = 0$) and put them into set F;

Step 2: for each individual j in the solution set F, determine its domination set S_j. Then, for individual k in the solution set S_j, execute the statement $n_k = n_k - 1$, which means that the number of solution individuals dominating individual k is subtracted by 1 (because individual j dominating individual k has been stored in the current set F). If $n_{\mathrm{k}} - 1 = 0$, then put individual k into another set H. The purpose of this step is to remove the influences of the individuals in the selected frontier and to facilitate the sorting of the remaining individuals;

Step 3: define the set F as the first nondominated set and mark the same nondominated sequence i_{rank} for each individual in set F;

Step 4: for the individuals in set H, repeat the above steps until all individuals are stratified.

(3) According to those objective functions, calculate the crowding distance of each individual in the nondominated layer according to Equation (12), and sort the internal individuals of each nondominated layer. To prevent the emergence of a local optimal solution, the lower the crowding degree is, the higher the nondomination degree is.

$$L(x_i) = \sum_{d=1}^{N} (f_d(x_{i+1}) - f_d(x_{i-1}))/(f_d^{\max} - f_d^{\min}) \tag{12}$$

In the formula, $f_d(x_{\mathrm{i}+1})$ and $f_d(x_{\mathrm{i}-1})$ are the dth objective function values of individuals $(i+1)$ and individuals $(i-1)$, respectively, $f_d^{\max}$ and $f_d^{\min}$ are the maximum and minimum values of the dth objective function for all individuals in the population, respectively.

(4) Use the elite strategy to remove substandard individuals according to the proportion set so that the superior individuals are carried into the next generation of optimization and obtain the final Pareto optimal solution through multiple iterations.

C. CALCULATION OF THE COMPROMISE SOLUTION

The optimized Pareto solution set can be obtained by the NSGA-II algorithm. To select the best compromise solution from the optimal solution set, fuzzy set theory is introduced. The steps are as follows:

Step 1: record the maximum value $F_i^{\max}$ and the minimum value $F_i^{\min}$ of the ith objective function in the Pareto optimal solution set.

Step 2: calculate the value u_i of the ith objective function corresponding to each Pareto solution by using Equation (13).

$$u_i = \begin{cases} 1 & \text{if } F_i \le F_i^{\min} \\ \dfrac{F_i^{\max} - F_i}{F_i^{\max} - F_i^{\min}} & \text{if } F_i^{\min} \le F_i \le F_i^{\max} \\ 0 & \text{if } F_i \ge F_i^{\max} \end{cases} \tag{13}$$

Step 3: based on Equation (14), calculate the normalized values of the membership functions for each nondominated solution in the Pareto optimal set.

$$u^k = \frac{\sum_{i=1}^{N} u_i^k}{\sum_{k=1}^{M} \sum_{i=1}^{N} u_i^k} \tag{14}$$

where N is the number of objective functions, and M is the number of nondominated solutions in the Pareto optimal set.

When the value u^{k} of each nondominated solution is calculated through the above steps in the Pareto optimal set, the best compromise solution of the multiobjective problem can be identified as the nondominated solution with the maximum value of u^{k}.

D. IMPROVEMENT STRATEGY FOR THE NSGA-II ALGORITHM

1) IMPROVEMENT OF THE PROPORTIONAL FACTOR IN THE SELECTION STRATEGY

The selection mechanism of the NSGA-II algorithm generally adopts the league selection method. In this selection rule, the two indexes for judging the quality of an individual are nondominated rank and crowding degree. In the same nondominated layer, the crowding degree of individual n is determined only by the difference between the objective function values of the two adjacent individuals; this makes the population diversity worse and further affects the optimization results. To reduce the number of repeat individuals and increase the diversity of the population, this paper improves the proportional factor set in the selection strategy. The rules are as follows:

$$\begin{aligned} C_m &= N_m{}^{*}\lambda_m, \quad m = 1, 2, \ldots, D_{\max} \\ \lambda_m &= z_m + \frac{k}{k_{\max}(x_m - z_m)} \end{aligned} \tag{15}$$

In (15), C_{m} is the number of individuals obtained from the mth nondominated layer of the selected population; N_{m} is the number of individuals in the mth nondominated layer; λ_{m} is the proportional factor; z_m and x_m are the variable parameters whose value range is [0.5,1] with $z_m < x_m$; k is the number of iterations; and $k_{\max}$ is the maximum number of iterations. The proportional factor λ_{m} is continuously adjusted according to the rank m of the nondominated layer. In this paper, z_m and x_m are only related to m, and their initial values are set as follows: $z_m = 0.5$ and $x_m = 1$. As m increase, z_m and x_m decrease at a rate of 0.01.

It should be noted that the proportional factor λ_{m} is a dynamic variable jointly determined by m and k. From the stratified sorting of the nondominated layer, the lower the rank in the nondominated layer is, the fewer the number of good individuals; furthermore, λ_{m} is decreasing with the increase of the rank m, and this can effectively reduce the number of disadvantaged individuals.

2) IMPROVEMENT OF THE CROSSOVER OPERATOR

The traditional NSGA-II algorithm generally uses a simulated binary crossover operator (SBX) to generate offspring; this limits the search range in some cases and may lead to instability in the evolution process. In this paper, to improve the convergence speed and reduce computational costs, the normal distribution crossover operator (NDX) is introduced into the crossover process, as it can effectively enhance the spatial search ability of the algorithm. Assuming that the parent generation contains P_1 and P_2 and their offspring generation contains Q_1 and Q_2, for the ith variable, the crossover process is as follows:

It generates a random number r ∈ (0, 1] when r < 0.5:

$$\begin{cases} Q_{1,i} = \dfrac{P_{1,i} + P_{2,i}}{2} + \dfrac{1.481(P_{1,i} - P_{2,i})\,|N(0,1)|}{2} \\ Q_{2,i} = \dfrac{P_{1,i} + P_{2,i}}{2} - \dfrac{1.481(P_{1,i} - P_{2,i})\,|N(0,1)|}{2} \end{cases} \tag{16}$$

When r > 0.5:

$$\begin{cases} Q_{1,i} = \dfrac{P_{1,i} + P_{2,i}}{2} - \dfrac{1.481(P_{1,i} - P_{2,i})\,|N(0,1)|}{2} \\ Q_{2,i} = \dfrac{P_{1,i} + P_{2,i}}{2} + \dfrac{1.481(P_{1,i} - P_{2,i})\,|N(0,1)|}{2} \end{cases} \tag{17}$$

where N (0,1) is a random variable with a normal distribution.

3) LOCAL CHAOTIC SEARCH STRATEGY

As the number of iterations increases, the NSGA-II algorithm is likely to fall into a local optimum due to the lack of diversity. To strengthen the local search ability of the NSGA-II algorithm, the local chaotic search strategy, which is used to explore higher-performance solutions around the individuals, is added into the improved NSGA-II algorithm after the offspring population is generated. There are two types of solutions for improved performance: (1) the new individual dominates the original one; (2) the new individual and the original individual do not dominate each other, but the fitness of the new individual is better than that of the original one. Thus, for an individual x, searching for a new individual x' in the neighborhood is the first step; then, if x' dominates x or its corresponding fitness value is better than that of the latter, the latter will be replaced; otherwise, continue the local chaotic search.

In the improved NSGA-II algorithm, for some elite individuals, using a local chaotic search strategy can make them tend to the Pareto frontier faster. For each individual, the following formula can be used to generate local search individuals.

$$x' = x + \frac{1}{k}(x^{\max} - x^{\min})(2L^k - 1)$$
$$L^k = \mu L^{k-1}(1 - L^{k-1}), \quad L^k \in [0, 1] \tag{18}$$

Among them, $x^{\max}$ and $x^{\min}$ are the upper and lower limits of the optimization variable x, k is the number of iterations, $L^{\mathrm{k}}$is the chaotic sequence generated by logistic mapping, μ represents the mapping coefficient, and L^{k} is the initial value (set to 4 in general) with a small difference ($\in$[0,1]). The adjacent search space will decrease with the increase of iterations.

V. APPLICATION OF INSGA-II TO THE MULTIOBJECTIVE OPTIMIZATION PROBLEM

A. CONSTRAINT CONDITION PROCESSING

When there is no constraint condition, it is assumed that x_1 and x_2 are two potential solutions of the multiobjective optimization problem. When at least one objective fitness value of x_1 is better than that of x_2, x_1 dominates x_2, and this is denoted as $x_1 \prec x_2$.

After adding constraints to the model, an unconstrained multiobjective evolutionary algorithm is infeasible. To solve this kind of constrained multiobjective optimization problem, constrained dominance is added to the Pareto dominance relationship [28].

Specifically, if a solution x satisfies the constraint condition it is called a feasible solution; otherwise, it is called an infeasible solution. For the infeasible solutions, a constraint violation value is used to describe the degree of violation of the constraints. For a solution x, the value can be expressed as follows:

$$CV(x_i) = \sum_{j=1}^{m} \langle g_j(x_i) \rangle + \sum_{k=1}^{l} |h_k(x_i)| \tag{19}$$

In the formula, $\langle \alpha \rangle$ represents that if $\alpha \leq 0$, then $\langle \alpha \rangle = 0$; otherwise, $\langle \alpha \rangle = |\alpha|$. Obviously, the smaller the CV value is, the better the solution. At the same time, for a feasible solution, the CV value is 0. In summary, the dominance relationship with constraints is defined as follows: for any two solutions x_1 and x_2, x_1 dominating x_2 needs to satisfy any of the following conditions:

$$\mathrm{CV}(x_1) = 0 \cap \mathrm{CV}(x_2) > 0 \tag{20}$$
$$\mathrm{CV}(x_1) > 0 \cap \mathrm{CV}(x_2) > 0 \cap \mathrm{CV}(x_1) < \mathrm{CV}(x_2) \tag{21}$$
$$\mathrm{CV}(x_1) = 0 \cap \mathrm{CV}(x_2) = 0 \cap x_1 \prec x_2 \tag{22}$$

B. ALGORITHMIC PERFORMANCE METRICS

To compare the performances of different algorithms, the spacing metric is introduced to evaluate the distribution of an algorithm's Pareto optimal solution set. The mathematical formula of the spacing metric is expressed as follows [29]:

$$S = \frac{\sum_{i=1}^{N-1} |d_{mean} - d_i|}{(N-1) \cdot d_{mean}} \tag{23}$$

where d_i represents the Euclidean distance between two adjacent individuals in the Pareto optimal solution set and d_{mean} represents the average distance among all Euclidean distances. N is the number of solutions in the Pareto optimal set. The smaller the value of the spacing metric is, the more evenly the Pareto optimal set is distributed.

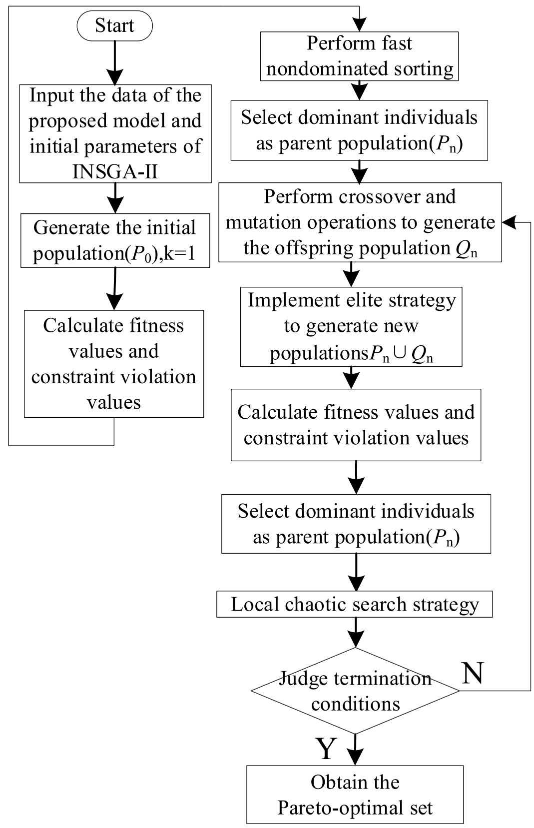

FIGURE 3. Flow chart of the model solution based on INSGA-II.

C. SPECIFIC SOLVING PROCESS OF INSGA-II

The steps of using the improved NSGA-II algorithm to solve the optimization model in this paper are as follows, and these steps are shown in Figure 3:

(1) Set the initial parameters of the algorithm and energy storage data.
(2) Randomly generate the initial population P_0 and set the number of iterations $k = 1$.
(3) Calculate the objective function value and constraint violation value of each individual in the current population.
(4) Perform fast nondominated sorting.
(5) Calculate the crowding degrees of the individuals in each nondominated layer according to the nondominated sorting results.
(6) Calculate the proportional factor and select the dominant individuals from the current population as the parent population P_{n}.
(7) Perform the crossover and mutation operations to generate the offspring population Q_{n}.

(8) Implement the elite strategy to generate new populations: $N_n = P_n \cup Q_n$.
(9) Calculate the fitness and constraint violation values of each individual in the current population.
(10) Perform fast nondominated sorting.
(11) Calculate the crowding degrees of the individuals in each nondominated layer according to the nondominated sorting results.
(12) Calculate the proportional factor and select the dominant individuals from the current population as the parent population P_n.
(13) Update P_n by using the local chaotic search strategy.
(14) Judge the termination conditions: if the number of iterations k reaches the maximum evolutionary algebra, then enter the next step; otherwise, return to step (7).
(15) Choose the optimal solution based on Equations (13) and (14).

According to Steps (1)- (15), the corresponding program is written in MATLAB to obtain the optimal configuration scheme for an ESS belonging to a prosumer.

VI. SIMULATION ANALYSIS

A. SIMULATION PARAMETERS

The simulation example of a prosumer is a cluster that consists of five users in a real science and technology park, and the basic data are shown in Table 1. All users installed photovoltaic roof systems with rated capacities from 10 kW to 30 kW. The operational data of the prosumer are selected on a typical day during the summer for simulation purposes. The initial value of the time-of-use price is shown in Table 4, and the energy storage parameters are shown in Table 5. The photovoltaic power generation curve of each user is shown in Figure 4, the original load curves are shown in Figure 5, and the total photovoltaic output and total load curves of the microgrid are shown in Figure 6. MATLAB 2016a is used to write the program for the algorithm in the Windows 10 system environment. The hardware system contains a CPU (Intel (R) Core (TM) i7-6500U) and RAM (8 GB).

TABLE 1. Basic data of all users.

User Name	Photovoltaic capacity/kW	Typical daily maximum load/kW
User1	10	17.328
User2	15	25.989
User3	20	24.61
User4	20	31.25
User5	25	38.58

B. OPTIMIZATION RESULTS AND ANALYSIS

The improved NSGA-II algorithm is used to solve the optimization model. The population size is set to 100, the maximum number of iterations is 100000, the crossover rate is 0.9, and the mutation rate is 0.1. To verify the superiority of INSGA-II, this paper compares its performance with those of other algorithms, such as SPEA2, NSGA-II and NSGA-III.

TABLE 2. Time-of-use prices.

Time	Microgrid's electricity price (RMB/kWh)	Feed-in tariff for PV (RMB/kWh)
02:00-10:00	0.551	0.4
24:00-02:00 10:00-15:00	0.88	0.4
15:00-24:00	1.21	0.4

TABLE 3. Simulation parameters of the ESS batteries.

Item	Value
Charging efficiency of all batteries	96%
Discharging efficiency of all batteries	96%
Minimal SOC of all batteries	10%
Initial SOC of all batteries	30%
Current energy storage price per kW	515RMB
Current energy storage price per kWh	1270RMB
Life cycle of energy storage devices	10 years
Discount rate	6%
Range of power capacity	[0 50]kW
Range of energy capacity	[0 500]kWh

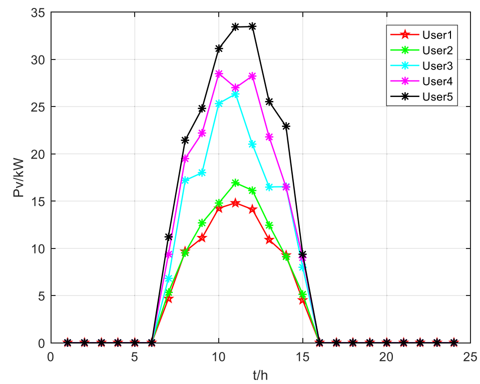

FIGURE 4. Photovoltaic output curves of all users.

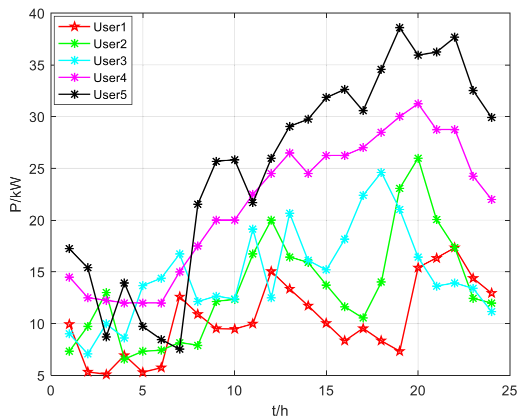

FIGURE 5. Original load curves of all users.

The Pareto frontiers of the different algorithms are calculated, as shown in Figure 7.

The Pareto distribution curves of the algorithms are similar. Compared with those of other algorithms, it is clear that the

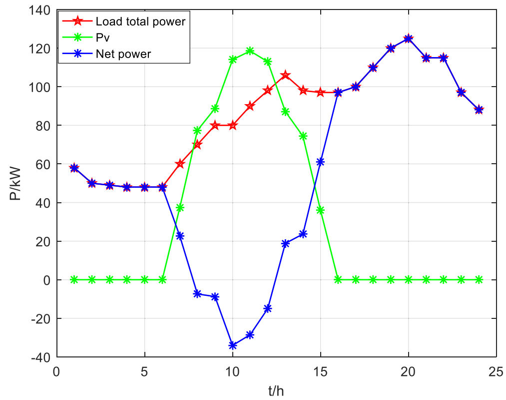

FIGURE 6. Total load and total photovoltaic output curves of all users.

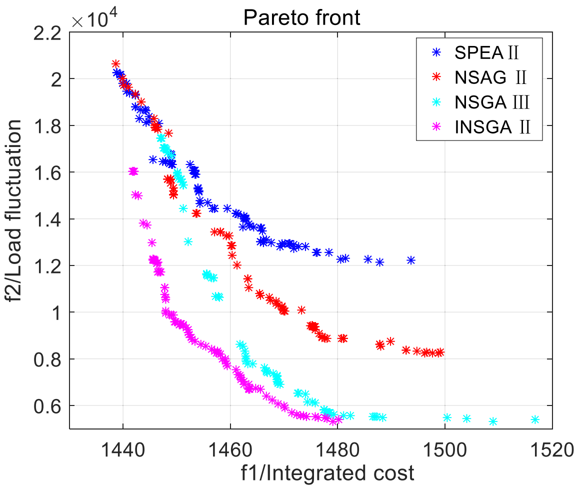

FIGURE 7. Comparison of Pareto fronts obtained by different algorithms.

corresponding Pareto optimal set of INSGA-II is significantly improved, and the quality of the solution is superior. Under the same comprehensive cost or load fluctuation, the solution obtained by INSGA-II is better than those of other algorithms.

1) COMPROMISE SOLUTIONS OF ALL ALGORITHMS

Table 4 shows the corresponding compromise solutions of the Pareto optimal solutions obtained by all compared algorithms. After configuring the ESS, the load fluctuations are greatly reduced. Comparing the results of these algorithms, the compromise solution of the proposed algorithm dominates the other solutions obtained by the other three algorithms. Furthermore, from the view of the calculation runtime, because the normal distribution crossover operator is introduced for the improved NSGA-II algorithm, the convergence speed is improved compared with that of NSGA-II. In summary, it is shown that the improvement strategies of NSGA-II are very successful.

2) ESS CONFIGURATION CORRESPONDING TO THE COMPROMISE SOLUTION

According to the compromise solution, the optimal capacity of the energy storage configuration is obtained. Capacity

TABLE 4. Comparison of the compromise solutions obtained by each algorithm.

Method	Composite cost/f1 (RMB)	Load fluctuation/f2	Runtime (s)
Unconfigured energy storage	1467.5	57312	
SPEA2	1454.281051	14631.78448	17.53
NSGA-II	1463.387826	11043.82779	16.53
NSGA-III	1463.3218	7802.103872	16.01
INSGA-II	1463.408145	6686.571631	14.53

TABLE 5. Energy storage capacity allocation corresponding to the Pareto compromise solution in each algorithm.

Meth od	Power capacit y (kW)	Energy capacity (kWh)	Total invest ment cost (RMB)	Operatio nal cost with ESS configura tion (RMB)	Total daily cost with ESS configura tion (RMB)
SPEA -II	76.374 65986	330.7682 624	534340	1255.377 951	1454.281 051
NSG A-II	83.772 20307	359.7537 734	581520	1246.923 426	1463.387 826
NSG A-III	83.533 313	395.8033 6	635470	1226.773 2	1463.321 8
INSG A-II	80.358 713	406.7879 1	650360	1221.317 045	1463.408 145

configuration results, energy storage investment costs and operating costs obtained by different algorithms are shown in Table 5, and the charging-discharging scheduling curves under all algorithms are shown in Figure 8.

From the results in Table 4 and Table 5, considering the life cycle of the energy storage device, the average daily total cost required after the configuration of the ESS is lower than that required without configuration. Theoretically, under the stimulation of electricity prices, the ESS of a prosumer reduces the electricity cost and load fluctuation to improve the operational stability of the microgrid through demand-side response.

From the scheduling curves obtained by each algorithm in Figure 8, when the ESS is not configured, the peak-to-valley difference reaches 159.01 kW; this is caused by the randomness of renewable energy output and load power. At the same time, renewable energy is only consumed by the actual load of the prosumer, and the consumption rate is 87.5%. After configuring the ESS for the prosumer, the new amount of energy can be consumed not only by the load but also by the ESS, and the photovoltaic consumption rates of the four algorithms reach 100%. Second, the orderly charging and discharging of the energy storage device is guided by the electricity price, and the peak-to-valley difference is greatly reduced compared with the original load curve; this improves the demand response and the comprehensive benefits of the prosumer. The peak-valley differences of the four algorithms are reduced to 93.6617 kW, 86.2423 kW, 111.4651 kW,

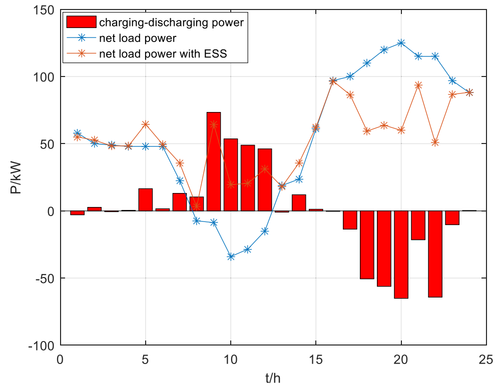

(a) Results obtained by SPEA-II.

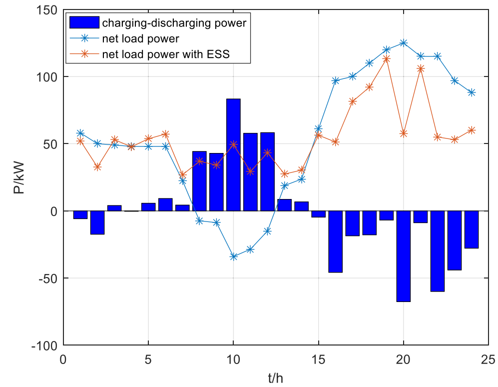

(b) Results obtained by NSGA-II.

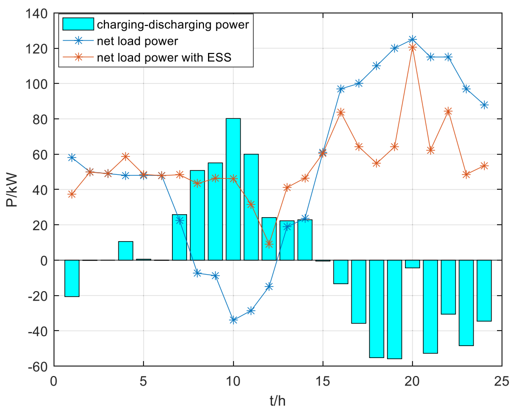

(c) Results obtained by NSGA-III.

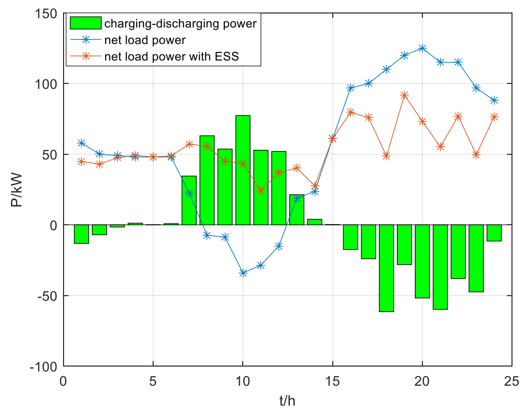

(d) Results obtained by INSGA-II.

FIGURE 8. ESS scheduling curve of the prosumer corresponding to the Pareto compromise solution obtained by each algorithm.

67.57 kW, and the lowest peak-valley difference is obtained by the improved NSGA-II algorithm.

Table 6 shows each algorithm's spacing metric value for the test system. It can be seen that INSGA-II has the minimum spacing metric value among the algorithms, and this indicates that the Pareto optimal solution set of INSGA-II is the most uniform distribution; furthermore, this illustrates that the effect of INSGA-II is the best among those of all algorithms.

TABLE 6. Spacing metric values of different algorithms.

INSGA-II	SPEA-II	NSGA-II	NSGA-III
0.9415	1.0555	1.2509	1.2687

To test the calculation stability of the INSGA-II algorithm in solving the multiobjective optimal model of the ESS configuration for a prosumer, this paper conducts multiple independent calculations on the INSGA-II algorithm and obtains the compromise solution corresponding to the Pareto optimal solutions in each calculation. In Figure 9, the histogram shows the compromise solution of two objective functions after running the algorithm ten times. The maximum values of the two objective functions for the compromise solution in ten trials are: composite cost = 1468.1576 RMB, load fluctuation = 6697.4218; the minimum values of the two objective functions are: composite cost = 1460.5469 RMB,

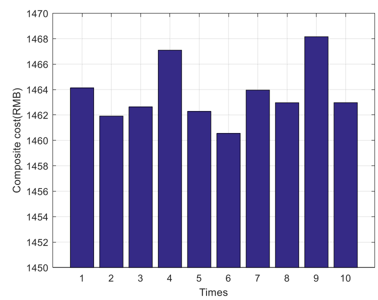

(a) Composite cost

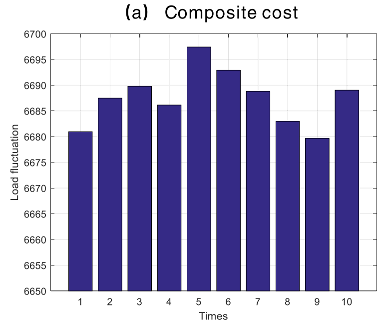

(b) Load fluctuation

FIGURE 9. The cylindrical figures of two objectives corresponding to the compromise solution of INSGA-II after running it ten times.

load fluctuation = 6679.6557; the average values of the two objective functions are: composite cost = 1463.6646 RMB, load fluctuation = 6687.5165; the standard deviations of these two objective functions are 2.3337 and 5.4149, respectively. From these data, it can be concluded that INSGA-II has strong calculation stability when solving the abovementioned model.

VII. CONCLUSION

In this paper, a multiobjective optimization model for ESS configuration is established by analyzing the scheduling mechanism of a prosumer. Considering the comprehensive cost and load fluctuation as the optimization objectives, the ESS capacity and charging-discharging scheduling are optimized according to the time-of-use price and load curves, and the problem is solved by the INSGA-II algorithm. Based on the traditional NSGA-II algorithm, the new algorithm improves the proportional factor in the selection strategy, and this can reduce the number of repeated individuals and increase the diversity of the population. At the same time, the crossover operator is improved, and the traditional binary crossover operator is replaced by the normal distribution crossover operator. Finally, a local chaotic search strategy is added to the algorithm. To test the effectiveness and superiority of the improved method, the original NSGA-II, SPEA2 and NSGA-III algorithms are used to compare the simulation results. By comparing the Pareto fronts obtained with various algorithms, the improved NSGA-II algorithm can find the best solution set, and the compromise solution is also better than the results obtained by other algorithms.To further verify the superiority of INSGA-II, the spacing metric is used to evaluate each algorithm's Pareto optimal set. The analysis shows that the corresponding Pareto optimal set of INSGA-II has a more even distribution than those output by other algorithms. Finally, this paper conducts ten independent calculations based on the INSGA-II algorithm. The performance results show that INSGA-II has strong robustness, and it is a very excellent method for solving the multiobjective optimization configuration problem of ESS for prosumers.

REFERENCES

[1] Y. Liu, X. Chen, Y. Wu, K. Yang, J. Zhu, and B. Li, "Enabling the smart and flexible management of energy prosumers via the energy router with parallel operation mode," *IEEE Access*, vol. 8, pp. 35038–35047, 2020.
[2] L. Park, Y. Yoon, S. Cho, and S. Choi, "Prosumer energy management considering contract with consumers under progressive pricing policy," *IEEE Access*, vol. 8, pp. 115789–115799, 2020.
[3] M. F. Zia, M. Benbouzid, E. Elbouchikhi, S. M. Muyeen, K. Techato, and J. M. Guerrero, "Microgrid transactive energy: Review, architectures, distributed ledger technologies, and market analysis," *IEEE Access*, vol. 8, pp. 19410–19432, 2020.
[4] C. D. Korkas, S. Baldi, I. Michailidis, and E. B. Kosmatopoulos, "Occupancy-based demand response and thermal comfort optimization in microgrids with renewable energy sources and energy storage," *Appl. Energy*, vol. 163, pp. 93–104, Feb. 2016.
[5] M. Marzband, F. Azarinejadian, M. Savaghebi, E. Pouresmaeil, J. M. Guerrero, and G. Lightbody, "Smart transactive energy framework in grid-connected multiple home microgrids under independent and coalition operations," *Renew. Energy*, vol. 126, pp. 95–106, Oct. 2018.
[6] M. Marzband, M. Javadi, S. A. Pourmousavi, and G. Lightbody, "An advanced retail electricity market for active distribution systems and home microgrid interoperability based on game theory," *Electr. Power Syst. Res.*, vol. 157, pp. 187–199, Apr. 2018.
[7] D. C. Korkas, S. Baldi, and B. E. Kosmatopoulos, "9 grid-connected microgrids demand management via distributed control and human-in-the-loop optimization," *Adv. Renew. Energies Power Technol.*, vol. 2, pp. 315–344, Mar. 2018.
[8] M. M. Iqbal, M. F. Zia, K. Beddiar, and M. Benbouzid, "Optimal scheduling of grid transactive home demand responsive appliances using polar bear optimization algorithm," *IEEE Access*, vol. 8, pp. 222285–222296, 2020.
[9] M. Ruiz-Cortes, E. Gonzalez-Romera, R. Amaral-Lopes, E. Romero-Cadaval, J. Martins, M. I. Milanes-Montero, and F. Barrero-Gonzalez, "Optimal charge/discharge scheduling of batteries in microgrids of prosumers," *IEEE Trans. Energy Convers.*, vol. 34, no. 1, pp. 468–477, Mar. 2019.
[10] C. H. Antunes, D. F. Pires, C. Barrico, Á. Gomes, and A. G. Martins, "A multi-objective evolutionary algorithm for reactive power compensation in distribution networks," *Appl. Energy*, vol. 86, nos. 7–8, pp. 977–984, Jul. 2009.
[11] X. Yuan, B. Zhang, P. Wang, J. Liang, Y. Yuan, Y. Huang, and X. Lei, "Multi-objective optimal power flow based on improved strength Pareto evolutionary algorithm," *Energy*, vol. 122, pp. 70–82, Mar. 2017.
[12] E. Zitzler, M. Laumanns, and L. Thiele, "SPEA2: Improving the performance of the strength Pareto evolutionary algorithm," *Parallel Problem Solving Nature-PPSN VIII*, vol. 3242, no. 4, pp. 742–751, Sep. 2004.
[13] Q. Zhang and H. Li, "MOEA/D: A multiobjective evolutionary algorithm based on decomposition," *IEEE Trans. Evol. Comput.*, vol. 11, no. 6, pp. 712–731, Dec. 2007.
[14] Y. Wang and Z. Cai, "Combining multiobjective optimization with differential evolution to solve constrained optimization problems," *IEEE Trans. Evol. Comput.*, vol. 16, no. 1, pp. 117–134, Feb. 2012.
[15] C. A. C. Coello and M. Reyes-Sierra, "Multi-objective particle swarm optimizers: A survey of the state-of-the-art," *Int. J. Comput. Intell. Res.*, vol. 2, no. 3, pp. 287–308, 2006.
[16] T. Q. Yang, "A multi-objective PSO algorithm for energy-efficient scheduling," *Adv. Mater. Res.*, vols. 143–144, pp. 663–667, Oct. 2010.
[17] Y. Guohua, Z. Xiangfen, M. Yujuan, H. Shijun, and W. Jinmei, "Capacity optimization of hybrid energy storage based on improved PSO algorithm," (in Chinese), *Electr. Meas. Instrum.*, vol. 52, no. 23, pp. 1–5, Dec. 2015.
[18] X. Wu, W. Cao, D. Wang, and M. Ding, "Multi objective optimization based on SPEA for the microgrid energy dispatch," in *Proc. 37th Chin. Control Conf. (CCC)*, Wuhan, China, Jul. 2018, pp. 7543–7548.
[19] T. Hao, G. Yang, P. Wang, L. Rui, L. Zhang, and J. Wang, "Capacity optimization of wind/solar hybrid power generation system based on improved differential evolution algorithm," (in Chinese), *J. Electr. Power Sci. Technol.*, vol. 32, no. 3, pp. 22–28, Mar. 2017.
[20] K. Deb, A. Pratap, S. Agarwal, and T. Meyarivan, "A fast and elitist multiobjective genetic algorithm: NSGA-II," *IEEE Trans. Evol. Comput.*, vol. 6, no. 2, pp. 182–197, Apr. 2002.
[21] N. Srinivas and K. Deb, "Muilti-objective optimization using non-dominated sorting in genetic algorithms," *Evol. Comput.*, vol. 2, no. 3, pp. 221–248, Mar. 1994.
[22] B. Y. Wang, H. Yin, and S. M. Zhang, "Research on algorithm of distributed reactive power optimization based on cloud computing and improved NSGA-II," *Appl. Mech. Mater.*, vols. 644–650, pp. 1927–1930, Sep. 2014.
[23] F. Ruiming, "Multi-objective optimized operation of integrated energy system with hydrogen storage," *Int. J. Hydrogen Energy*, vol. 44, no. 56, pp. 29409–29417, Nov. 2019.
[24] R. Sathishkumar, V. Malathi, and V. Premka, "Optimization and design of PV-wind hybrid system for DC micro grid using NSGA II," *Circuits Syst.*, vol. 7, no. 7, pp. 1106–1112, Jul. 2016.
[25] B. Ye, X. Shi, X. Wang, and H. Wu, "Optimisation configuration of hybrid AC/DC microgrid containing electric vehicles based on the NSGA-II algorithm," *J. Eng.*, vol. 2019, no. 10, pp. 7229–7236, Oct. 2019.
[26] A. G. Azar, H. Nazaripouya, B. Khaki, C.-C. Chu, R. Gadh, and R. H. Jacobsen, "A non-cooperative framework for coordinating a neighborhood of distributed prosumers," *IEEE Trans. Ind. Informat.*, vol. 15, no. 5, pp. 2523–2534, May 2019.
[27] S. A. El-Batawy and W. G. Morsi, "Optimal design of community battery energy storage systems with prosumers owning electric vehicles," *IEEE Trans. Ind. Informat.*, vol. 14, no. 5, pp. 1920–1931, May 2018.

[28] B. Ji, X. Yuan, and Y. Yuan, "Modified NSGA-II for solving continuous berth allocation problem: Using multiobjective constraint-handling strategy," *IEEE Trans. Cybern.*, vol. 47, no. 9, pp. 2885–2895, Sep. 2017.
[29] R. Tavakkoli-Moghaddam, M. Azarkish, and A. Sadeghnejad-Barkousaraie, "A new hybrid multi-objective Pareto archive PSO algorithm for a bi-objective job shop scheduling problem," *Expert Syst. Appl.*, vol. 38, no. 9, pp. 10812–10821, Sep. 2011.

FEI LI was born in Yichang, Hubei, China, in 1986. He received the M.S. degree in electrical engineering from China Three Gorges University, in 2011, where he is currently pursuing the Ph.D. degree. From 2011 to 2013, he worked as a Design Engineer with Guiyang Engineering Corporation Ltd. From 2013 to 2019, he was a Research Assistant with the Hubei Provincial Key Laboratory of Operation and Control of Cascade Hydropower Station. His research interests include power system operation and control, hydropower station simulation operation, and microgrid optimization scheduling.

XIANSHAN LI received the Ph.D. degree in electronics and systems from Blaise Pascal University, France, in 2004. He is currently a Professor with China Three Gorges University. His research interests include power system operation and control, hydropower station simulation operation, and microgrid optimization scheduling.

BINQIAO ZHANG received the Ph.D. degree in electrical engineering from the Huazhong University of Science and Technology, Wuhan, China, in 2017. He is currently an Associate Professor with China Three Gorges University. His research interests include the optimal operation of energy Internet and operation simulation of hydropower station.

ZHENXING LI received the Ph.D. degree in electrical engineering from the Huazhong University of Science and Technology, Wuhan, China, in 2013. He is currently an Associate Professor with China Three Gorges University. His research interests include protective relaying and power system stability control.

MINGFANG LU is currently pursuing the Ph.D. degree with China Three Gorges University, Yichang, China. Her research interests include power system operation and control, hydropower station simulation operation, and microgrid optimization scheduling.